P_0 Glycoprotein Overexpression Causes Congenital Hypomyelination of Peripheral Nerves

Lawrence Wrabetz,* Maria Laura Feltri,* Angelo Quattrini,* Daniele Imperiale,*‡ Stefano Previtali,* Maurizio D'Antonio,* Rudolf Martini,§ Xinghua Yin,‖ Bruce D. Trapp,‖ Lei Zhou,¶ Shing-Yan Chiu,¶ and Albee Messing**

*Department of Neurology and Department of Biological and Technological Research (DIBIT), San Raffaele Scientific Institute, 20132 Milano, Italy; ‡First Division of Neurology, University of Torino, 10126 Torino, Italy; §Department of Neurology, Section of Developmental Neurobiology, University of Wurzburg, Wurzburg, Germany; ‖Department of Neurosciences, Lerner Research Institute, Cleveland Clinic Foundation, Cleveland, Ohio 44195; ¶Department of Physiology, School of Medicine, University of Wisconsin-Madison, Madison, Wisconsin 53706; and **Waisman Center and Department of Pathobiological Sciences, School of Veterinary Medicine, University of Wisconsin-Madison, Madison, Wisconsin 53705

Abstract. We show that normal peripheral nerve myelination depends on strict dosage of the most abundantly expressed myelin gene, *myelin protein zero* (*Mpz*). Transgenic mice containing extra copies of *Mpz* manifested a dose-dependent, dysmyelinating neuropathy, ranging from transient perinatal hypomyelination to arrested myelination and impaired sorting of axons by Schwann cells. Myelination was restored by breeding the transgene into the *Mpz*-null background, demonstrating that dysmyelination does not result from a structural alteration or Schwann cell-extrinsic effect of the transgenic P_0 glycoprotein. *Mpz* mRNA overexpression ranged from 30–700%, whereas an increased level of P_0 protein was detected only in nerves of low copy-number animals. Breeding experiments placed the threshold for dysmyelination between 30 and 80% *Mpz* overexpression. These data reveal new points in nerve development at which Schwann cells are susceptible to increased gene dosage, and suggest a novel basis for hereditary neuropathy.

Key words: axon sorting • myelin • neuropathy • Schwann cell • transgene

Introduction

The myelin sheath displays a unique molecular architecture that depends on precisely regulated protein synthesis and trafficking. First, myelinating glia, Schwann cells in peripheral nerve, and oligodendrocytes in brain and spinal cord, must solve a remarkable problem of quantity: to produce as much as three times their weight in proteins and lipids per day of myelinogenesis (Norton and Poduslo, 1973). Coordinate synthesis of myelin proteins is in part transcriptionally mediated, as high-level transcription of the genes encoding myelin-specific proteins is induced simultaneously during myelinogenesis (Stahl et al., 1990; Scherer et al., 1994; Wrabetz et al., 1998). Second, the trafficking of these mRNAs and proteins is carefully regulated. For example, in myelin-forming Schwann cells, P_0 glycoprotein (P_0)[1] is synthesized in the RER, and trafficked via the Golgi apparatus specifically to the forming myelin sheath (D'Urso et al., 1990; Trapp et al., 1995). In contrast, the mRNA encoding myelin basic protein (MBP) is trafficked to cytoplasmic spaces adjacent to the forming myelin sheath, where MBP is synthesized on free ribosomes and rapidly incorporated into myelin (Colman et al., 1982; Trapp et al., 1987; Griffiths et al., 1989).

It is not surprising, therefore, that both naturally occurring and induced mutations reveal the importance of precisely regulated gene dosage for normal myelination. For example, the gain or loss of only one allele of the proteo-

Lawrence Wrabetz and Maria Laura Feltri contributed equally to this work.

Address correspondence to Lawrence Wrabetz, San Raffaele Scientific Institute, DIBIT, Via Olgettina 58, 20132 Milano, Italy. Tel.: 39-02-26434870. Fax: 39-02-26434767. E-mail: l.wrabetz@hsr.it

[1]*Abbreviations used in this paper:* $^{+/-}$, heterozygous; CHN, congenital hypomyelination neuropathy; CMAP, compound muscle action potential; CMT1A, Charcot-Marie-Tooth 1A neuropathy; CNS, central nervous system; F80, founder 80; GAPDH, glyceraldehyde-3-phosphate dehydrogenase; MBP, myelin basic protein; *Mpz*, *myelin protein zero* gene; NCV, nerve conduction velocity; nt, nucleotide; P, postnatal day; P_0, P_0 glycoprotein; PLP, proteolipid protein; PMP22, peripheral myelin protein 22 kD; RT, reverse transcription; Tg80, transgenic line 80.

lipid protein gene (*PLP*), or peripheral myelin protein 22 kD gene (*PMP22*), produce central nervous system (CNS) myelinopathies or demyelinating peripheral neuropathies in human (for reviews see Suter and Snipes, 1995; Nave and Boespflug-Tanguy, 1996), and similar dosage alterations of *Plp* and *Pmp22* in transgenic rodents model these diseases (*Plp*: Boison and Stoffel, 1994; Kagawa et al., 1994; Readhead et al., 1994; Klugmann et al., 1997; and *Pmp22*: Adlkofer et al., 1995; Magyar et al., 1996; Sereda et al., 1996; Huxley et al., 1998). How altered PLP expression causes dysmyelination is unclear (for review see Werner et al., 1998), but overexpressed PMP22 arrives to the myelin sheath (Vallat et al., 1996), possibly destabilizing its formation or maintenance. The observation that mutations in diverse myelin genes produce similar disease phenotypes implies that various myelin proteins interact in functional units. In keeping with this, physical interaction between PMP22 and P_0 has been detected in myelin (D'Urso et al., 1999) supporting that multiprotein assemblies reside within the myelin sheath. Thus, destabilization of myelin formation due to altered myelin gene dosage may reflect a need for stringent stoichiometry during protein trafficking to, and assembly of, the myelin sheath.

P_0 mRNA ($\sim$8% of total mRNA) and protein ($>$50% of peripheral myelin protein; Greenfield et al., 1973) are by far the most abundant in nerve. P_0 is a single-pass transmembrane protein with an extracellular immunoglobulin-like domain, and a cytoplasmic tail enriched in basic residues (Lemke and Axel, 1985; Shapiro et al., 1996). The extracellular domain of P_0 participates in homophilic interactions (D'Urso et al., 1990; Filbin et al., 1990; Schneider-Schaulies et al., 1990; Shapiro et al., 1996), which mediate compaction of the extracellular space between spirals of Schwann cell plasma membrane during myelin formation, as demonstrated by uncompaction of myelin in mice that lack P_0 (Giese et al., 1992). Phenotypes due to P_0 overexpression have not been identified, but gene duplications rather than nulls are increasingly appreciated as a mechanism for genetic disease, especially for myelin genes. For example, duplication of chromosomal segments containing *PLP* or *PMP22* cause Pelizeaus-Merzbacher Disease (Nave and Boespflug-Tanguy, 1996) or Charcot-Marie-Tooth 1A neuropathy (CMT1A; Suter and Snipes, 1995), respectively.

Since P_0 is the most abundant protein in peripheral myelin, and serves an analogous function to PLP in central myelin, we sought to explore the phenotypic consequences of overexpressing P_0 using transgenic techniques. Our data show that *myelin protein zero* (*Mpz*) gene dosage must be precisely regulated, as overexpression of P_0 causes a dose-dependent, dysmyelinating neuropathy manifested by remarkably delayed nerve development, including Schwann cells that are unable to segregate axons. Thus far, we have identified two possible pathogenetic mechanisms. First, increasing P_0 overexpression disregulates the stoichiometric expression of other myelin genes. Second, P_0 overexpression promotes inappropriate trafficking of P_0 to Schwann cell surface membranes (Yin et al., 2000, this issue). These findings have implications for both coordinate expression and trafficking of myelin proteins in developing nerve, and for dosage dependent human neuropathies, such as CMT1A.

Materials and Methods

Production of Transgenic Mice

Construction of the transgenic vector mP_0TOTA has been described previously (Feltri et al., 1999). Like mP_0TOTA, mP_0TOT contains the complete *Mpz* with 6 kb of promoter, all exons and introns, the natural polyadenylation site, and a polymorphic BglII site in exon 3 (amino acid sequence conserved) that is absent from the endogenous FVB/N *Mpz* alleles. In contrast to mP_0TOTA, the ATG start site of translation of P_0 remains. For oocyte injection, the transgene monomer was excised from the vector using XhoI and NotI.

Transgenic mice were obtained by standard techniques (Brinster et al., 1985) using fertilized eggs obtained from the mating of FVB/N mice (Taconic). Breeding lines of animals were maintained by backcrosses to FVB/N mice (Taconic or Charles River). Ten founders were identified by Southern blot and PCR analysis of genomic DNA prepared from tail samples (Sambrook et al., 1989). We documented expression in eight founders or their progeny; these were further analyzed in this study. A 770-nucleotide (nt) BamHI–HindIII restriction fragment from intron 1 of *Mpz* was used to generate a probe for Southern blot analysis of genomic DNA digested with BglII (Fig. 1). As endogenous and transgenic P_0 alleles are recognized identically by this probe, copy numbers were determined by the quotient of the 2.8-kb divided by the 6.8-kb band intensity in Southern blot analysis. The PCR primer sequences were: 5′-CCACCACCTCTCCATTGCAC-3′ and 5′-GGCGGATTGACCGTAATGGG-3′, and amplified a 540-nt fragment. BglII digestion of the product revealed additional fragments of 300 and 240 nt in transgenic samples (data not shown). PCR conditions were: 94°C for 30 s, 57°C for 60 s, and 72°C for 60 s (25 cycles), followed by 10 min extension at 72°C, in a standard PCR reaction mix. The genetic designations of the three lines that have been maintained

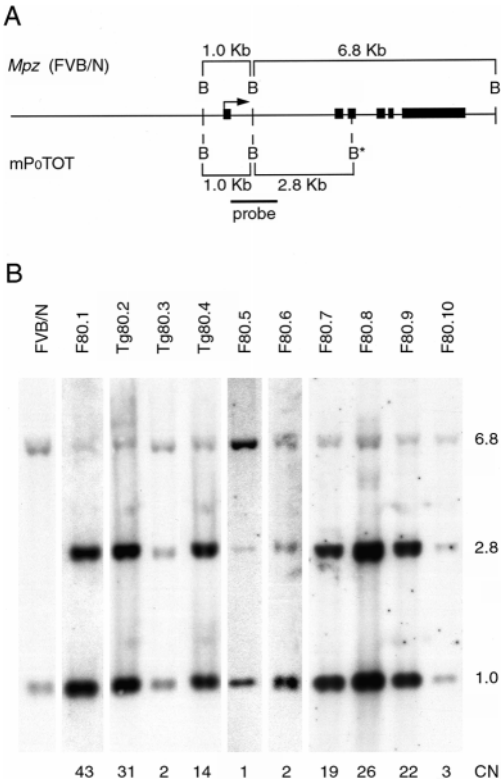

Figure 1. Southern blot analysis for transgene copy number. Southern blot analysis (B) revealed ten founders (F80), from which three lines were established (Tg80). A polymorphic BglII restriction site (B*) distinguishes the mP_0TOT transgene from the endogenous *Mpz* FVB/N alleles (A). Copy numbers (CN) were estimated by the ratio of the 2.8–6.8-kb signal intensities.

from this study are transgenic lines: 80.2, TgN(Mpz)22Mes; 80.3, TgN (Mpz)23Mes; and 80.4, TgN(Mpz)24Mes.

P_0 heterozygous ($^{+/-}$) null mice were backcrossed to FVB/N mice for five generations and identified by PCR or Southern blot analysis of genomic DNA prepared from tail samples. The PCR primer sequences were: 5′-TCAGTTCCTTGTCCCCCGCTCTC-3′ (forward, common), 5′-GGCTGCAGGGTCGCTCGGTGTTC-3′ (reverse, neo) and 5′-ACTTGTCTCTTCTGGGTAATCAA-3′ (reverse, wild-type P_0), and amplified a 500-nt fragment from a wild-type allele and a 334-nt fragment from the null allele. Multiplex PCR conditions were 94°C for 60 s, 53°C for 180 s, and 72°C for 180 s (40 cycles), followed by 10 min extension at 72°C, in a standard PCR reaction mix.

Tg80.4 and $P_0^{+/-}$ animals were crossed to generate breeders for the rescue experiments. Southern blot analysis as for Tg80 (above) distinguished genotypes of offspring (see Fig. 8).

Behavioral Analysis

Tremor was estimated visually on a + to ++++ scale. Strength was measured in the forelimbs of adult mice using a Grip Strength Meter (Columbus Instruments). In brief, mice were tested five consecutive times over a span of about one min, recording peak force applied to the strain gauge (in g). The maximum value achieved in the five tests was taken as an indication of strength and used for further calculations. To account for possible weakness due to muscle atrophy rather than strictly neural conduction deficits, strength was expressed as a ratio of the maximal peak force over body weight. The investigator performing the tests was blinded to the genotype of each mouse. As grip strength/weight declined slightly with age in normal controls, all reported measurements derive from littermates between postnatal day 90 (P90) and P110.

Electrophysiologic Analysis

Transgenic mice and control littermates at P42 were anesthetized by i.p. injection of avertin, and the sciatic nerve and gastrocnemius muscle were exposed and continuously perfused with Ringer's solution at room temperature. The compound muscle action potential (CMAP) was measured extracellularly by a blunt tip glass pipette as the sciatic nerve was supramaximally stimulated with a bipolar stimulation electrode connected to a Grass stimulator. To evaluate the nerve conduction velocity (NCV), the nerve stimulation electrode was moved between two fixed sites on the nerve separated by a known distance. The NCV was calculated as the distance divided by the time shift of the CMAP expressed in m/s. In parallel, mice were killed by decapitation, and the sciatic nerves quickly excised and placed in a nerve chamber at a bath temperature of 20°C. The compound nerve action potential was recorded by a tight suction electrode at the cut end of the nerve. Supramaximal brief stimulation (50 V, 0.01 ms) was given to elicit action potentials. NCV was evaluated by measuring the distance between the stimulating site and the recording site. The NCV determined from muscle and nerve action potentials coincided, eliminating the motor endplate as a source of delay. For Tg80.2, the amplitude of nerve action potentials was reduced relative to control (0.94 ± 0.208 [3] versus 3.03 ± 1.353 [3]), but the number of points were too few to show statistical significance by *t* test ($P \sim 0.15$).

Morphological Analysis

Hematoxylin and eosin, and ATPase isozyme (pH 4.6 or 9.4) staining of posterior compartment muscles of the leg was performed according to standard clinical laboratory protocols. ATPase (pH 9.4) staining confirmed the presence of angulated fibers and the absence of fiber type grouping (not shown).

Routine semi-thin section and electron microscopic analyses of nerve was performed as described (Quattrini et al., 1996). In most cases, nerves from three to five animals were evaluated at each time point for each line of Tg80. When only founders were available, both sciatic as well as femoral nerves were evaluated. To account for variable genetic background in rescue experiments (performed in FVB/N N(2–5)F1 background), three to five animals of each genotype were evaluated by four investigators blinded to the genotype. Each genotype produced a highly reproducible phenotype.

Quantitation of myelinated fibers in developing motor (quadriceps) versus sensory (saphenous) branches of femoral nerve was performed as described (Frei et al., 1999).

The proportion of myelinated fibers in semi-thin section analysis of P28 sciatic nerve (Table I) was estimated by the proportion of axons in a 1:1 relationship with a Schwann cell that also contained myelin, as counted in three independent transverse sections.

Semiquantitative Reverse Transcription PCR (RT-PCR)

Sciatic nerves were dissected from FVB/N, BALB/c (BALB/c Ahn; Harlan), transgenic, and nontransgenic littermates and total RNA was prepared as described (Feltri et al., 1999). The RT-PCR assay was performed as described (Feltri et al., 1999). To verify that the method was quantitative, known amounts (based on RT-PCR analysis for total P_0 from each) of wild-type FVB/N (not containing the DpnII polymorphism) or BALB/c (containing the DpnII polymorphism) sciatic nerve RT products were mixed in various proportions, and analyzed as above (see Fig. 7 B). Note that the polymorphic BglII site (Fig. 1) becomes a DpnII site in the transgenic cDNA.

Northern Blot Analysis

Total RNA was isolated from mouse sciatic nerves and from various tissues by $CsCl_2$ gradient centrifugation (Chirgwin et al., 1979). Northern blot analysis was performed as described (Feltri et al., 1999), using cDNAs of mouse P_0, rat MBP, and rat glyceraldehyde-3-phosphate dehydrogenase (GAPDH) to generate probes.

Western Blot Analysis

Frozen sciatic nerves dissected from P28 transgenic and nontransgenic littermates were pulverized, sonicated in lysis buffer (95 mM NaCl, 25 mM Tris-HCl, pH 7.4, 10 mM EDTA, 2% SDS, and protease inhibitors), boiled for 5 min, and spun at 14,000 rpm in a microcentrifuge for 10 min at room temperature to eliminate insoluble material. The protein in supernatants was determined by BioRad protein assay according to the manufac-

Table I. Behavioral, Electrophysiological, and Morphological Phenotype Parallel Tg80 Copy Number and Expression

	Wild-type	Tg80.3	Tg80.4	Tg80.2
Copy number	0	2	14	31
Fold overexpression*	0	0.3	0.8	7.3
Median life-span	>2 yr	>2 yr	10 mo	4 mo
Tremor	−	−	++	++++
Grip strength‡ (males)	4.7 ± 0.28 (10)	5.0 ± 0.06 (3)	4.6 ± 0.20 (2)	1.4 ± 0.14 (3)§
Grip strength‡ (females)	5.7 ± 0.30 (16)	5.8 ± 0.45 (2)	5.0 ± 0.01 (2)	1.9 ± 0.15 (3)§
NCV (m/s)	36 ± 4.3 (5)	ND	11 ± 4.0 (4)§	2 ± 0.1 (3)§
Percent myelinated fibers‖	100	100	50	<10

*Age of analyses: expression, tremor, and percent myelinated fibers at P28; grip strength at ~P100; NCV at P42.
‡Grip strength = absolute grip strength (g)/body weight (g).
§$P < 0.01$ by *t* test as compared with wild-type.
‖The percent of axons in 1:1 relationships with Schwann cells that are myelinated.

turer's instructions. Equal amounts of homogenates (containing 2.5–10 μg of protein) were brought up to 5 μl with 8 M urea, to which was added 5 μl of 8 M urea, 0.05 M DTT, 1%SDS in water, followed by 10 μl of standard reducing sample buffer. The samples were denatured, resolved on a 12% SDS-polyacrylamide gel, and electroblotted onto PVDF membrane. Preliminary experiments with increasing amounts of wild-type nerve homogenates between 2.5 and 10 μg determined the linear range of dose-response for each of tubulin, MBP, PMP22, and P_0. To verify equal loading of protein, membranes were stained with amido black or ponceau red. Parallel blots were blocked with 0.05% Tween, 5% dry milk in PBS, and incubated with the appropriate antibody in 0.05% Tween and 1% dry milk in PBS. Mouse mAbs recognized P_0 ($P_0$7, the generous gift of Dr. Juan Archelos, Department of Neurology, Karl-Franzens-Universitat, Graz, Austria; Archelos et al., 1993), MBP (Boehringer Mannheim), PMP22 (the generous gift of Dr. Ueli Suter, Swiss Federal Institute of Technology, Zürich, Switzerland), and β-tubulin (Sigma Chemical Co.). Peroxidase-conjugated secondary antibodies (Sigma Chemical Co.) were visualized using the ECL method with autoradiography film (Pharmacia Biotech). The intensity of bands was quantified by densitometry, and the ratio of intensities for each myelin protein and β-tubulin was determined. Many blots were checked directly for equal loading by amido black staining after antibody experiments were completed. Deglycosylation with PNGase F and endoglycosidase H was performed on homogenates per manufacturer's instructions (New England Biolabs). mAb $P_0$7 recognized two bands of M_r 28,500 and 22,000–24,000, as previously noted in rodent nerve by Archelos et al. (1993), who speculated that the lower band was a degraded form of P_0. Deglycosylation analysis of either transgenic or wild-type P28 nerve lysates showed that both bands contained a mixture of endoglycosidase H-sensitive and -resistant (immature and mature, respectively) forms of P_0, as previously reported by Brunden (1992) for adult nerve.

Because both Northern and Western analysis of sciatic nerves pooled from ten Tg80.3 or ten normal littermates at P28 underestimated the decrease in MBP expression seen by Western analysis performed on pairs of nerves from single animals, we hypothesized that Tg80.3 animals manifested some combination of incomplete penetrance or variable expressivity for reduced MBP expression. Western blot analysis for P_0 and MBP normalized to tubulin on multiple pairs of nerves confirmed incomplete penetrance, as 40% of Tg80.3 animals showed P_0 overexpression as compared with the mean of the normal littermates, and each animal with P_0 overexpression showed an ~50% reduction of MBP (for example, see Fig. 9).

Taqman® Quantitative RT-PCR Analysis

Quantitative RT-PCR was performed as per manufacturer's instructions (Taqman®, PE Applied Biosystems Instruments) on an ABI PRISM 7700 sequence detection system (Applied Biosystems Instruments), using total RNA prepared as above from P28 sciatic nerves. The relative standard curve method was applied using total RNA from wild-type littermate sciatic nerves as the reference. Tg80.3 and wild-type determinations were carried out in separate tubes for both P_0 mRNA and GAPDH mRNA. RT was performed as above. PCR amplification was performed with input RT product corresponding to 0.5 ng of starting RNA. PCR conditions were: 50°C for 2 min, 95°C for 10 min, followed by 95°C for 15 s, 60°C for 1 min for 40 cycles in TaqMan® universal master reaction mix. Primers included: P_0 forward, 5′-GTCCAGTGAATGGGTCTCAGATG-3′; P_0 reverse, 5′-CTTGGCATAGTGGAAAATCGAAA-3′; GAPDH forward, 5′-TGCACCACCAACTGCTTAG-3′; and GAPDH reverse, 5′-GGATGCAGGGATGATGTTC-3′. Probes included: P_0 FAM-5′-ACCTGGCGCTACCAGCCTGAAGG-3′-TAMRA; and GAPDH JOE-5′-CAGAAGACTGTGGATGGCCCCTC-3′-TAMRA. This analysis revealed that P_0 mRNA was increased 0.68 ± 0.27, $n = 3$ (mean ± SEM) in Tg80.3 relative to wild-type, which agrees reasonably well with 0.3-fold overexpression by semiquantitative RT-PCR analysis of the level of Tg80.3 mRNA relative to endogenous P_0 mRNA, and 60% overexpression of P_0 by Western analysis.

Results

Extra Copies of Mpz Cause Dysmyelination in Peripheral Nerve

To overexpress P_0 we employed the mP_0TOT transgene (Tg80), which contains the entire *Mpz* gene and 6 kb of 5′ flanking sequence (Fig. 1). mP_0TOT containing the *lac*Z reporter gene embedded in *Mpz* exon 1 was previously shown to be expressed specifically in myelin-forming Schwann cells in postnatal peripheral nerve, in parallel with endogenous *Mpz* (Feltri et al., 1999). We prepared transgenic mice by standard techniques and obtained ten founders. Four manifested wobbling gait and tremor and were unable to breed. We were able to establish only one line from these severely affected mice by in vitro fertilization from the founder 80.2, and we subsequently maintained this line by ovarian transplantation. The remaining six founders manifested little or no tremor; two of these transmitted the transgene to progeny (hereafter, F80 denotes founder animals, whereas Tg80, animals of a line; e.g., F80.2 or Tg80.2). Southern blot analysis showed that copy number ranged from 1 to >40 (Fig. 1).

F80.1, F80.8, F80.9, and Tg80.2 animals (all copy number >20) showed a severe phenotype including gait difficulty, reduced weight, tremor, atrophy of the paraspinal and hindlimb musculature (Fig. 2 A), and reduced lifespan (Table I). Nerve conduction velocities in the Tg80.2 animals were profoundly reduced to ~2 m/s with temporal dispersion of the compound motor action potential (Fig. 2 B) suggesting a dysmyelinating neuropathy. Morphological analysis of leg muscles showed angulated and atrophic fibers suggestive of denervation, but no fiber type group-

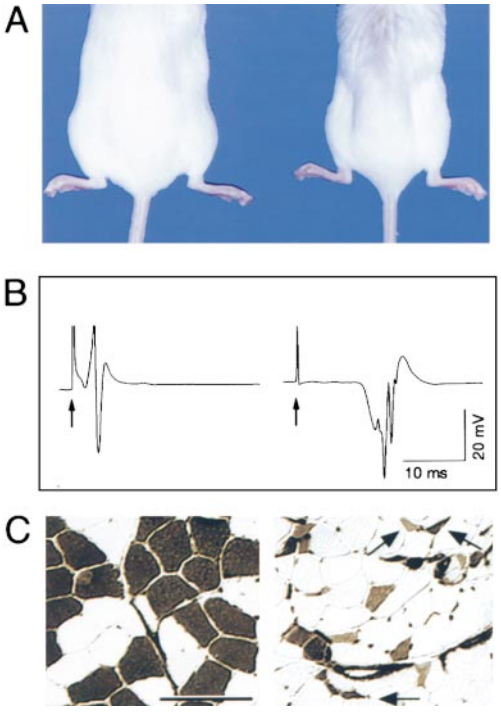

Figure 2. Phenotype of high copy number Tg80.2 animals. A, Tg80.2 animals at P120 manifested atrophy in axial and hindlimb muscles. B, Traces are shown of CMAP generated by sciatic nerve stimulation in P42 animals. Arrows indicate stimulation artifact. Note the markedly delayed onset and dispersion of the Tg80.2 CMAP, due to the slowed NCV. C, ATPase isotype staining (pH 4.6) in leg muscles revealed atrophy of many fibers and angulated fibers (arrows), suggesting denervation. Bar, 100 μm.

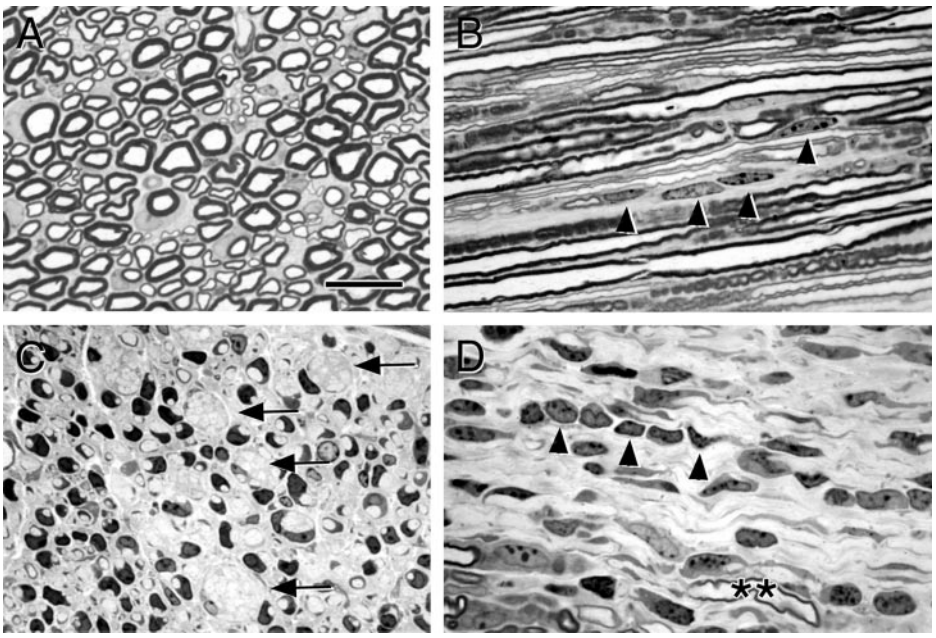

Figure 3. Semi-thin section analysis of sciatic nerve in Tg80.2. Transverse (A and C) or longitudinal (B and D) sections stained with toluidine blue from P28 Tg80.2 (C and D) as compared with wild-type (A and B) sciatic nerves showed a marked paucity of myelin (one internode of thin myelin is marked by a double asterisk) and an increased number of nuclei (arrowheads). In addition, bundles of unsorted axons surrounded by several Schwann cell nuclei were evident in every section (arrows; see also Fig. 4). No onion bulbs were seen. Bar, 20 μm.

ing to suggest nerve regeneration. These data were consistent with a severe dysmyelinating neuropathy with secondary effects on neurons.

Morphological analysis of high copy number animals confirmed severe dysmyelination with rare evidence of myelin destruction. Semi-thin section analysis of P28 sciatic nerve from Tg80.2 animals showed remarkable hypomyelination and an increase in the number of Schwann cell nuclei (Fig. 3). Occasional patches of myelinated fibers were seen at P28 (Fig. 3) and more frequently at P42 (data not shown). Electron microscopic analysis of these nerves showed a mixture of fibers with thin myelin sheaths for the diameter of axon, and fibers in which single Schwann cells ensheathed axons, but formed no myelin (Fig. 4). Within the perineurial compartment, collagen was increased. There was little evidence of active demyelination as myelin debris was not seen extracellularly or in macrophages. Periodicity appeared normal in the few thin myelin sheaths present (Fig. 4, inset). Nonmyelin-forming (Remak) Schwann cells with apparently normal ensheathment and segregation of small axons could be found (Fig. 4). No axonal degeneration was observed.

Remarkably, in each transverse section of sciatic nerve at P28, several families of Schwann cells associated with bundles of naked axons of mixed caliber were identified (Fig. 3 C, arrows). Ultrastructural analysis (Fig. 4) revealed that nerve development was arrested at the stage in which Schwann cells were segregating large axons away from these bundles. Normally these bundles disappear from rodent sciatic nerve in the first few days after birth. Many other large axons were associated with, but only partially ensheathed by, a single Schwann cell surrounded by many pockets of redundant basal lamina containing collagen. Very rarely, single naked axons surrounded by a basal lamina were seen (data not shown). These data suggested that Schwann cells had incompletely retracted their processes after segregation of large axons. The unsorted bundles of axons did not depend on the site of chromosomal insertion of Tg80.2, as they were also present in F80.1 and F80.8, and very rarely in Tg80.4 animals. These features all suggested a perinatal effect of increased *Mpz* gene dosage.

Dysmyelination Results from Developmental Delay

To confirm that the defect in myelination resulted from developmental delay, and not myelin destruction, we examined nerves at various postnatal ages. In contrast to controls, Tg80.2 sciatic nerves at P5 and P14 contained virtually no myelin (Fig. 5). Also, the axon-sorting defect was more evident at P5 and P14 than at P28 by both semi-thin section analysis (compare Figs. 5 and 3) and EM (data not shown). Even in P45 or P90 transgenic nerves some bundles of unsorted larger diameter axons remained (Fig. 5). To quantitate the lack of myelin formation, we examined the motor branch (quadriceps) of developing femoral nerve as previously described (Frei et al., 1999). By P10, $<1\%$ of axons in 1:1 relationships with Schwann cells were myelinated in Tg80.2 nerve, whereas virtually 100% of such axons were myelinated in wild-type nerve (Table II). A very low level of demyelination was detected in quadriceps nerves, as occasional degenerating myelin fragments could be seen within axons or Schwann cells at P10. Thus, the abnormal features of P28 nerves resulted primarily from developmental delay, not from destruction of myelin that had been synthesized earlier, although some fibers acquired myelin by adulthood.

The occasional thinly myelinated fibers were not distributed randomly in transverse sections of sciatic nerve. One possibility was that motor and sensory fibers were differentially affected, since fibers originating from single spinal roots are also nonrandomly distributed in sciatic nerve (Ueyama, 1978). Consistent with this idea, the motor branch (quadriceps) was more dysmyelinated than the sensory branch (saphenous) of femoral nerve by P10 in Tg80.2 animals (Table II). In addition, ventral roots were

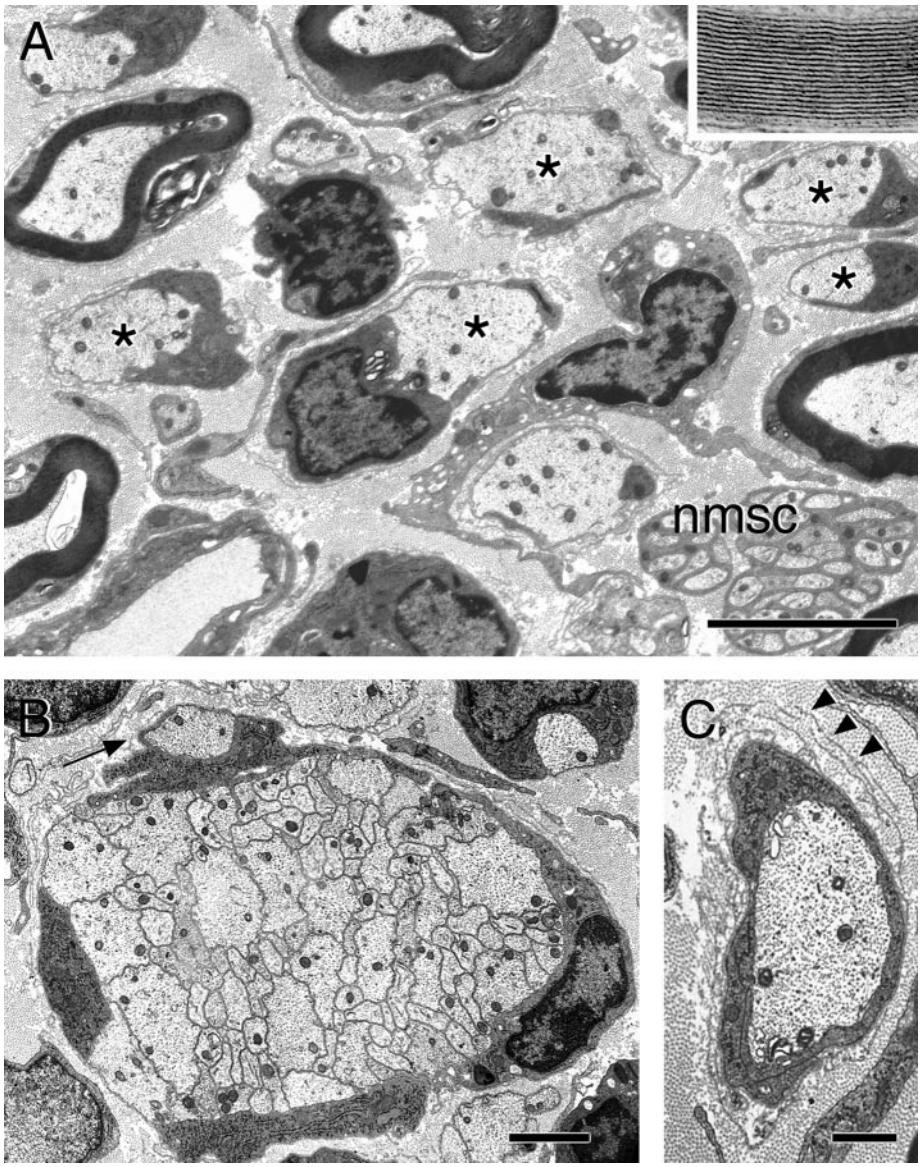

Figure 4. Ultrastructural analysis of Tg80.2 sciatic nerve showed dysmyelination. A, A typical transverse section of P28 sciatic nerve showed a mixture of occasional Schwann cells that had formed thin myelin sheaths of normal periodicity (inset), or more commonly, Schwann cells that had ensheathed single large axons, but had not advanced an inner mesaxon around them (asterisks). Nonmyelinforming Schwann cells (nmsc) ensheathed small axons normally. Bar, 5 μm. B, Other Schwann cell families surrounded bundles of mixed caliber, naked axons; some of these Schwann cells were segregating large axons away from the bundles (arrow). Bar, 2 μm. C, Many Schwann cells were surrounded by pockets of redundant basal lamina, some containing collagen fibers (arrowheads). Bar, 1 μm.

more markedly dysmyelinated than dorsal roots in both Tg80.2 (Yin, X., unpublished results) and Tg80.3 homozygotes (see below; Quattrini, A., unpublished results). Thus, as in several other rodent models (reviewed in Martini, 1997), motor fibers are relatively more dysmyelinated than sensory fibers in Tg80 mice.

Dysmyelination Parallels Mpz Dosage and Overexpression

The increasing severity of the behavioral, electrophysiological, and morphological phenotype paralleled increasing transgene copy number (Table I; Fig. 6). For example, animals with 0–10 copies (Tg80.3, F80.10) appeared behaviorally normal, and had normally myelinated nerves by P28 (Fig. 6 B). In contrast, animals with 10–20 copies (Tg80.4 and F80.7) manifested mild tremor, NCV of 11m/s (Tg80.4), and dysmyelination with ~50% of the large axons ensheathed by single Schwann cells that had not formed myelin (Fig. 6 C). Finally, animals with >20 copies (Tg80.2, F80.1, F80.8, and F80.9) manifested evident tremor, weak grip strength, conduction velocity of 2 m/s (Tg80.2), and severe hypomyelination along with delayed axonal sorting (Fig. 6, E and F).

Thus, we performed RT-PCR analysis to confirm that the severity of phenotype paralleled *Mpz* overexpression. Primers that recognized exons 2 and 3 of *Mpz*, flanking a polymorphic restriction site in exon 3, allowed us to distinguish and quantitate the transgenic relative to endogenous P_0 mRNA. We standardized the assay by analyzing mix-

Table II. Percent of Myelinated Fibers in Motor and Sensory Branches of P10 Femoral Nerve

	Tg80.2	Wild-type
	%	%
Quadriceps	<1	100
Saphenous	5–10	70

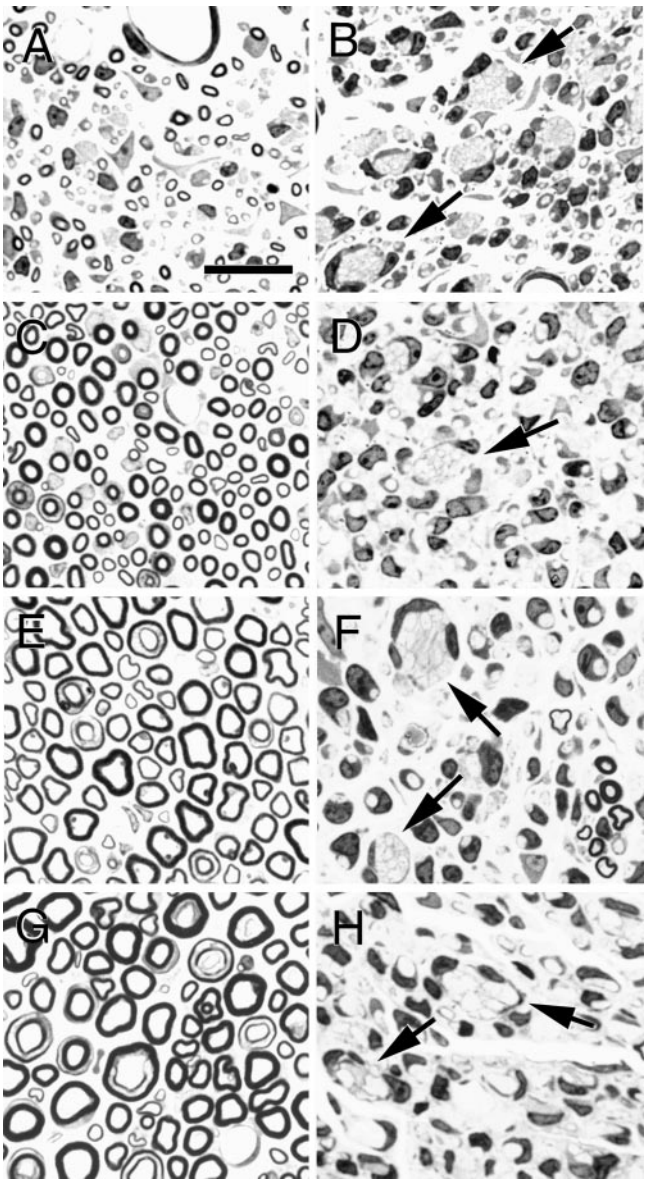

Figure 5. Semi-thin section analysis of Tg80.2 sciatic nerves during postnatal development. Transverse sections stained with toluidine blue from wild-type (A, C, E, and G) or Tg80.2 (B, D, F, and H) animals at P5 (A and B), P15 (C and D), P45 (E and F), and P90 (G and H) demonstrate that dysmyelination was already present by P5 and remained throughout development. Arrows indicate bundles of unsorted axons. Extracellular myelin debris was not obvious at any age (see also Fig. 4). Bar, 50 μm.

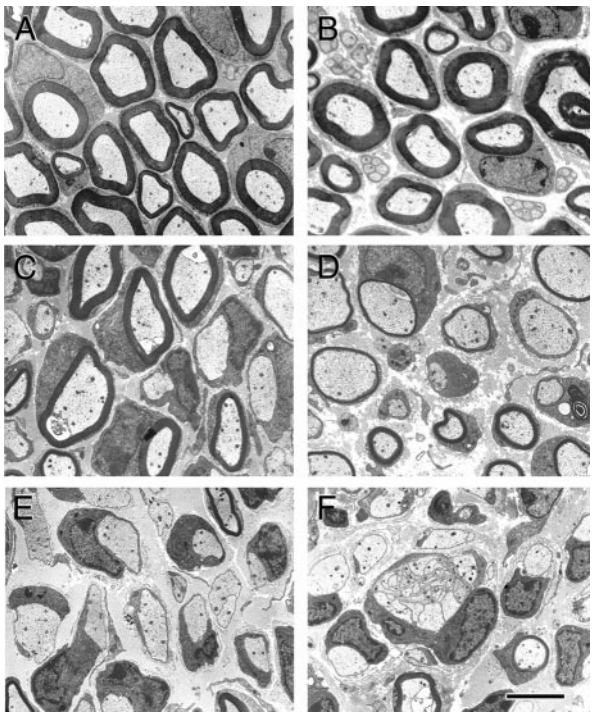

Figure 6. Dysmyelination parallels *Mpz* gene dosage. Low magnification electron micrographs of transverse sections of P28 sciatic nerve from FVB/N (A), Tg80.3 (B), Tg80.4 (C), Tg80.3 homozygote (D), Tg80.2 (E), and F80.8 (F) demonstrate that dysmyelination was absent in low copy number animals (B), moderate in middle copy number animals (C), and most pronounced in high copy number animals (E and F). Note that in contrast to Tg80.3 hemizygotes (B), Tg80.3 homozygotes manifested dysmyelination (D). Bar, 5 μm.

tures of known amounts of cDNAs reverse-transcribed from sciatic nerve mRNA of BALB/c or FVB/N mice, the strains from which Tg80 or the endogenous *Mpz* gene derived, respectively. As shown in Fig. 7 B, the assay produced proportions within ±5% of the starting amounts. Analyzing mRNA from P28 sciatic nerves of Tg80.2, Tg80.3, or Tg80.4 animals, we found that *Mpz* was overexpressed from 30 to ~700%. Overexpression paralleled copy number, and severity of phenotype, among the categories of low, medium, and high copy number (Table I).

To show that *Mpz* was overexpressed shortly after birth, the point in development at which myelination was delayed, we performed RT-PCR analysis on Tg80.2 sciatic nerves at P2. We found that the ratio of Tg80 to endogenous *Mpz* was 6.9-fold at P2, very similar to 7.3-fold determined at P28 (Fig. 7 C). This data, taken together with the demonstration by ultrastructural immunocytochemistry that P_0 is significantly increased in periaxonal, abaxonal, and Golgi membranes of arrested Tg80.2 Schwann cells at P5 (see Figure 3 of Yin et al., 2000, this issue), shows that P_0 overexpression is associated with congenital hypomyelination in sciatic nerve.

In the mildly affected Tg80.3, dysmyelination was related to the expression of endogenous *Mpz*. As *Mpz* expression approaches its peak between P15 and P21 (Stahl et al., 1990), Tg80.3 sciatic nerves were hypomyelinated (thin sheaths for axon diameter) as compared with control (data not shown), whereas by P28, when *Mpz* expression is falling to adult levels, sciatic nerves contained ultrastructurally normal myelin (Fig. 6 B). Thus, we hypothesized that total *Mpz* expression in Tg80.3 sciatic nerves had exceeded a threshold at P15, above which hypomyelination results. To directly identify such a threshold, we bred Tg80.3 to homozygosity. P28 Tg80.3 homozygotes manifested tremor and dysmyelination (Fig. 6 D), whereas P28 80.3 hemizygotes did not (Fig. 6 B). RT-PCR analysis confirmed an increase in overexpression from 30% in Tg80.3

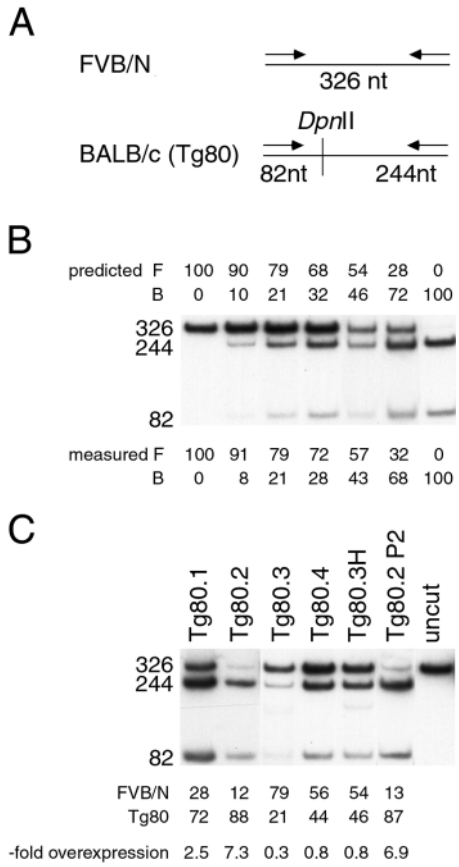

Figure 7. Semiquantitative RT-PCR analysis reveals *Mpz* overexpression. A, Total RNA prepared from sciatic nerve was reverse-transcribed; the product was amplified by PCR using a primer pair that recognized identically both endogenous (FVB/N) or Tg80 (BALB/c) P_0 cDNAs. The FVB/N cDNA was distinguished by DpnII digestion, revealing 244- and 82-nucleotide (nt) products. B, Various mixtures of FVB/N (F) and BALB/c (B) reverse-transcribed product were analyzed to validate the method. The relative proportion (in percent of total signal) of FVB/N (326-nt band) or BALB/c (244 + 82-nt bands) were ± 5% of predicted in three separate experiments (one shown). C, Reverse-transcribed products from sciatic nerve total RNA from various transgenic nerves at P28 or P2 (Tg80.2 P2) were analyzed for the relative proportion of Tg80 P_0 mRNA. Overexpression (-fold) was the quotient of Tg80 signal divided by endogenous signal. Note that the pairs, Tg80.4 and Tg80.3H (homozygote) or Tg80.2 P28 and Tg80.2 P2, manifested very similar ratios of overexpression. Undigested amplification product (uncut) revealed only the 326-nt band.

hemizygote nerves to 80% in Tg80.3 homozygote nerves (Fig. 7 C). Of note, the effects of *Mpz* overexpression were reproducible between transgenic lines, as the behavioral and morphologic phenotypes of Tg80.3 homozygotes (80% overexpression) and Tg80.4 animals (80% overexpression) were similar (compare Fig. 6, C and D). These data confirm that the severity of dysmyelination depends on *Mpz* dosage.

To further confirm this relationship, and that dysmyelination did not depend on ectopic expression or a structural alteration of Tg80, the converse experiment was performed by breeding Tg80.4 into the *Mpz* null background. As compared with Tg80.4 (Fig. 8 B), Tg80.4 in the heterozygous null background produced more myelin in sciatic nerve, showing a mixture of hyper- and hypomyelinated fibers (Fig. 8 F). When Tg80.4 was bred into the homozygous null background, myelination returned to essentially normal (Fig. 8 D), consistent with the prediction that total *Mpz* expression should decrease from 180% in Tg80.4 animals to near normal in Tg80.4/homozygous *Mpz* null animals. These data demonstrate that a threshold exists for *Mpz* overexpression between 30 and 80% (130–180% total *Mpz* expression), above which dysmyelination results. More importantly, in the absence of endogenous *Mpz*, Tg80.4 generated P_0 sufficient to form normal myelin sheaths. Therefore, the overexpression phenotype depends uniquely on dosage of *Mpz*, not on an ectopic effect or structural alteration of transgenic P_0.

P_0 Glycoprotein Is Overexpressed

To determine whether increased dosage of *Mpz* and expression of P_0 mRNA resulted in overexpression of P_0, we performed Western blot analysis. In Tg80.3 nerves at P28, where nerves were ultrastructurally normal (Fig. 6 B), P_0 was overexpressed by ~60% (Fig. 9; 0.6 ± 0.16, $n = 5$ [mean ± SEM]), as predicted by the RT-PCR analysis. Increased total P_0 mRNA was sufficient to explain this increase, as confirmed by Taqman® quantitative RT-PCR analysis: total P_0 mRNA in Tg80.3 sciatic nerves was increased 0.68 ± 0.27, $n = 3$. Of note, as *Mpz* overexpression rose further, the level of P_0 fell, corresponding to more severe dysmyelination: it was slightly less than control in Tg80.4, and significantly reduced in Tg80.2. Thus, as P_0 overexpression exceeds a threshold leading to dysmyelination, mRNA and protein levels diverge, as protein levels reflect primarily the bulk quantity of P_0 in myelin sheaths. P_0 deriving from the transgene could not be distinguished from endogenous P_0 (including deglycosylation with PNGase F or endoglycosidase H, followed by Western blot analysis, data not shown) suggesting that the transgenic protein underwent normal posttranslational modification. In keeping with this, ultrastructural immunocytochemical analysis showed that the few myelin sheaths seen in P42 Tg80.2 ventral roots contained 40% more grains for P_0 as compared with control sheaths (see Figure 4 of Yin et al., 2000, this issue). Thus, at least some of the extra P_0 probably arrived to myelin sheaths.

P_0 Overexpression Is Accompanied by Dysregulated Expression of other Myelin Genes, even in the Absence of Dysmyelination

To examine for possible effects of P_0 overexpression on the synthesis of other myelin proteins in the presence of normal myelination or dysmyelination, we performed Western blot analysis on P28 sciatic nerves from animals of low (Tg80.3), medium (Tg80.4), or high (Tg80.2) copy number. As for P_0, the level of MBP was reduced in association with the loss of bulk myelin in Tg80.4 and Tg80.2 nerves. In addition, higher molecular weight isoforms of MBP, which in the CNS are associated with early myelinogenesis (Barbarese et al., 1978), were predominant in Tg80.4 and Tg80.2, consistent with developmental delay, whereas the 18-kD isoform, most abundant in mature CNS myelin

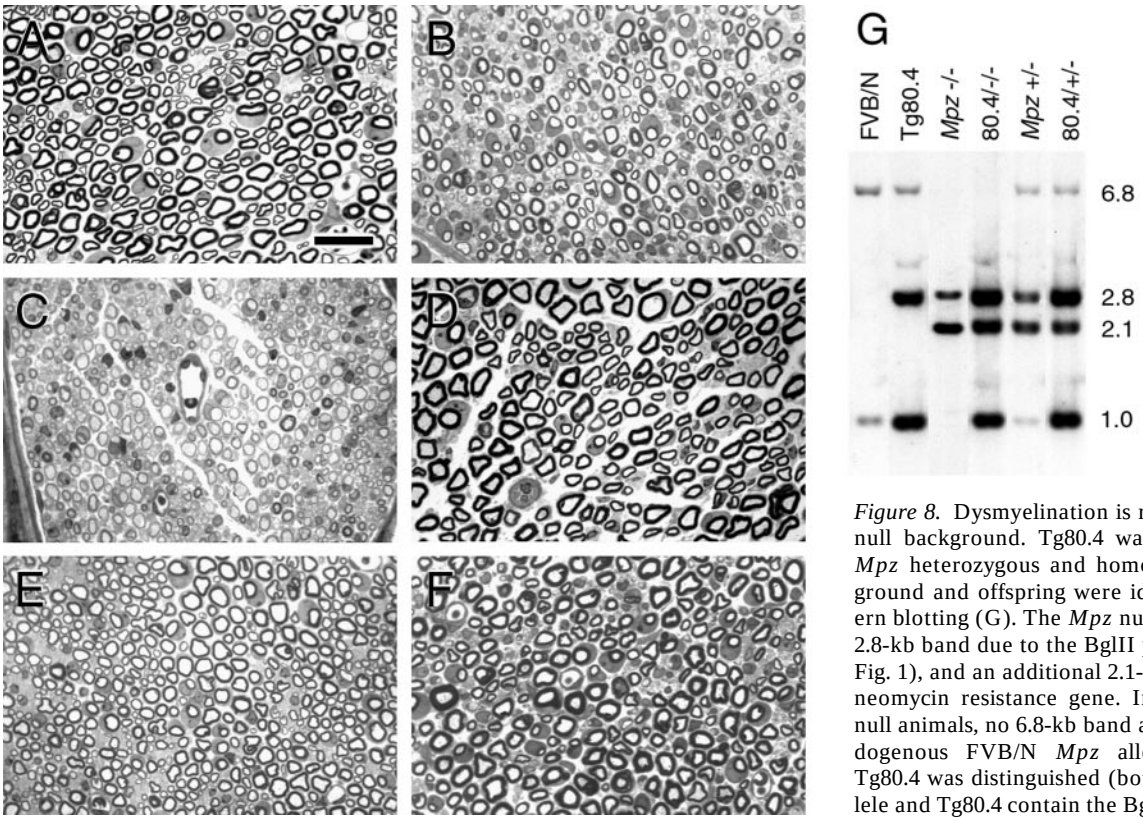

Figure 8. Dysmyelination is rescued in the *Mpz* null background. Tg80.4 was crossed into the *Mpz* heterozygous and homozygous null background and offspring were identified by Southern blotting (G). The *Mpz* null allele produced a 2.8-kb band due to the BglII polymorphism (see Fig. 1), and an additional 2.1-kb band due to the neomycin resistance gene. In the homozygous null animals, no 6.8-kb band appeared as the endogenous FVB/N *Mpz* alleles were absent. Tg80.4 was distinguished (both the *Mpz* null allele and Tg80.4 contain the BglII polymorphism) by the presence of a much more intense 1.0-kb band. Semi-thin section analysis of P28 sciatic nerves from 3–5 animals of each genotype showed that Tg80.4 homozygous null nerves (80.4/$^{-/-}$; D) appeared normally myelinated as compared with nontransgenic (FVB/N; A) littermates, and as compared with the dysmyelinated Tg80.4 (B) or homozygous null (*Mpz*$^{-/-}$; C) littermates. Note that at P28, heterozygous null (*Mpz*$^{+/-}$; E) littermates were slightly hypomyelinated in the FVB/N congenic background, and that Tg80.4 heterozygous null nerves (80.4/$^{+/-}$; F) showed a mixture of hypo- and hypermyelinated fibers. Bar, 20 μm.

sheaths, was predominant in Tg80.3 and the control. Surprisingly, the MBP level was reduced by ~50% in P28 Tg80.3 sciatic nerves as compared with control (Fig. 9; 0.52 ± 0.05, $n = 5$), in the absence of myelin abnormality (Fig. 6 B). PMP22 was also reduced by 35% in Tg80.3 (0.37 ± 0.16, $n = 2$), but was equal to, or twofold increased in Tg80.2 and Tg80.4 nerves, respectively (Fig. 9). The level of a nonmyelin protein, tubulin, was not altered. P_0 overexpression thus perturbed myelin protein levels in not only the presence, but also the absence of dysmyelination, where the reduced levels of proteins cannot be explained by the loss of bulk myelin.

Since P_0 accounts for >50% of protein in peripheral myelin (Greenfield et al., 1973), and thus represents the bulk of protein in nerve lysates, overexpression of P_0 might artifactually cause a reduction in the amount of other proteins detected in Western blots. For instance, overexpression of P_0 by 60% might be expected to increase total nerve protein by ~30%, and if the expression of other proteins remains unchanged, their proportion of total nerve protein would be reduced by 25%. To control for this possibility, amido black staining of blots revealed that proteins other than P_0 or MBP (easily recognized in amido black staining, see Fig. 9) were equally loaded between Tg80.3 and control (Fig. 9). Moreover, the reduction in MBP was 50%, significantly >25%, and therefore, out of proportion to changes in total protein due to P_0 overexpression. Thus, Schwann cells sense and respond to P_0 overexpression by dysregulating other myelin proteins before exceeding a threshold for dysmyelination.

Discussion

We have shown that myelinogenesis requires expression of the P_0 within a narrowly defined range. Our data are most consistent with a model in which overexpressing P_0 results in dose-dependent arrest of nerve development, ranging from transient hypomyelination with mild overexpression, to arrest of Schwann cells in a 1:1 relationship with large axons with moderate overexpression, to inability of Schwann cells to segregate axons with the highest overexpression. This array of phenotypes suggests multiple pathogenetic mechanisms, some acting before and some during myelin formation. We have identified two plausible mechanisms: the first involves altered trafficking of P_0 in promyelin-forming Schwann cells (Yin et al., 2000, this issue), and the second involves abnormal stoichiometry in the expression of myelin genes. These studies reveal new stages in nerve development at which Schwann cells are susceptible to altered gene dosage and suggest that P_0 overexpression represents a new mechanism of hereditary neuropathy.

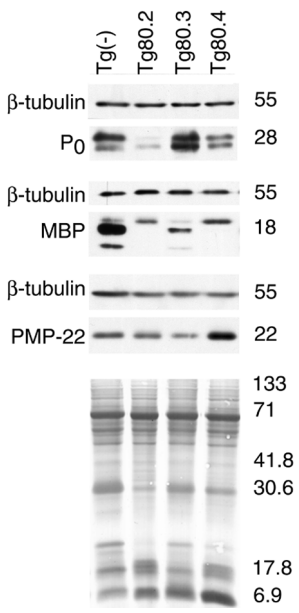

Figure 9. P_0 overexpression is accompanied by alteration of other myelin protein levels. Western blot analysis was performed on P28 sciatic nerve lysates from Tg80 animals with dysmyelination ranging from none (Tg80.3), to moderate (Tg80.4), to severe (Tg80.2). Dysmyelination was associated with proportionally decreased total P_0, and high molecular weight isoforms of MBP consistent with developmental delay. In contrast, Tg80.3 nerves showed ~60% increased P_0 and mature MBP isoforms. Note that MBP and PMP22 levels were reduced in Tg80.3 nerves, even when normalized to tubulin or amido black staining of the blot for total protein. Numbers × 1,000 indicate approximate M_r.

The phenotypes observed in P_0 transgenic mice do not arise from structural alteration or ectopic expression of the transgenic protein. First, a version of mP_0TOT containing *lacZ* embedded in exon 1 expressed the reporter with the same cell-specific and developmental profile as *Mpz* (Feltri et al., 1999). Moreover, in the present study, the ratio of transgenic to endogenous P_0 mRNA remained stable from P2 (Fig. 7) through adulthood (Wrabetz, L., unpublished result). Second, Western blot analysis of multiple independent lines revealed that the transgenic and endogenous P_0 proteins were indistinguishable, even by deglycosylation analysis. Most importantly, when the P_0 transgene (Tg80.4 line) was bred into the homozygous P_0 null background, normal myelination resulted, even though all P_0 was transgenic in origin. The sum of this data strongly supports the view that the phenotype of P_0 transgenics derives from increased dosage and expression of *Mpz* in Schwann cells.

Schwann Cell Response to P_0 Overexpression Is Specific

Dysmyelination might represent a nonspecific response to glycoprotein overexpression. However, even though Schwann cell development is arrested by altered dosage of several genes related to myelination (some encoding glycoproteins), specific morphological features distinguish each phenotype (*Mpz*, Giese et al., 1992; *Pmp22*, Adlkofer et al., 1995; Magyar et al., 1996; Sereda et al., 1996; Huxley et al., 1998; *Oct6*, Bermingham et al., 1996; Jaegle et al., 1996; *Krox20*, Topilko et al., 1994). In particular, developmental arrest at the stage of sorting large caliber axons from bundles of naked axons is unique to P_0 overexpression, suggesting an effect early in nerve development. The data from Yin et al. (2000, this issue) demonstrate that even common morphological features belie specific Schwann cell dysfunction. Schwann cells arrested in a 1:1 relationship with axons in P_0 transgenic mice have narrowed mesaxonal spaces, whereas the same cells in PMP22 overexpressor mice do not (compare Figure 6 in Yin et al., 2000, this issue, to Figure 7 in Huxley et al., 1998). Finally, we report that mistrafficking of P_0 in the P_0 transgenic mice does not disrupt sorting of myelin-associated glycoprotein into appropriate subcellular compartments (Yin et al., 2000, this issue), indicating that glycoprotein trafficking is not generally impaired.

Dose Dependence and Mechanisms of Developmental Arrest

The phenotype resulting from P_0 overexpression is dose-dependent. As copy number and the level of transgenic mRNA rise, the behavioral and electrophysiological phenotype worsen, and the proportion of appropriately myelinated fibers falls (Fig. 6; Table I). Breeding the Tg80.3 line (30% overexpression) to homozygosity produced dysmyelination similar to hemizygous Tg80.4 mice with comparable levels of expression (Fig. 7 C). Conversely, crossing the Tg80.4 transgene into the homozygous P_0 null background (predicted normalized P_0 levels) produced normal myelination (Fig. 8). These experiments place the threshold for dysmyelination between 30 and 80% P_0 overexpression. It is important to note that the phenotype of P_0 overexpression is one of dysmyelination, not demyelination. Study of early development in Tg80.4 (not shown) and Tg80.2 mice (Fig. 5) demonstrates that myelin is never properly formed in affected fibers, not that myelin is formed and then destroyed.

As a general rule, as *Mpz* dosage rises, Schwann cells are progressively impaired. Thus, we observed three categories of abnormal Schwann cells in P_0 overexpressor nerves: 1, Schwann cells that formed thin myelin; 2, Schwann cells arrested after having ensheathed a large axon and advanced a mesaxon; and 3, Schwann cells arrested as they attempted to sort axons. Nerves with low P_0 overexpression (e.g., Tg80.3) have only the first type of Schwann cells; nerves with moderate overexpression (e.g., Tg80.4) have primarily the first and second type of Schwann cells; nerves with highest overexpression (e.g., Tg80.2) have all three types.

It is important to note that our quantitation of P_0 overexpression is at the level of whole nerve, whereas the heterogeneity of phenotypes in individual cells suggests variation in either the level of transgene expression or susceptibility to dysmyelination. Interestingly, we observed that motor nerves and ventral roots were more severely affected than sensory nerves and dorsal roots in the P_0 transgenics. In fact, semiquantitative in situ hybridization analysis for P_0 mRNA on teased fibers from sciatic nerves shows that Schwann cells associated with larger fibers express more P_0 (Griffiths et al., 1989). Perhaps motor fibers, which are larger than sensory fibers on the average, have a stronger stimulus to express both endogenous and transgenic P_0, and therefore more quickly achieve levels of P_0 overexpression sufficient to arrest Schwann cell development. Similarly increased susceptibility of Schwann cells associated with motor axons to dysmyelination has been observed with mutations or dosage alterations of *Pmp22*, *Mpz*, *Mag*, and *Cx32* (Martini, 1997).

More than one mechanism may account for these Schwann cell abnormalities in P_0 overexpressor nerves.

For example, nerves of the Tg80.3 line at P28, with ultrastructurally normal myelin, manifest a 50% increase of P_0 protein in combination with reduced levels of two other myelin proteins, MBP and PMP22. Preliminary analysis suggests that these alterations are reflected in part by changes in mRNA levels (Wrabetz, L., and M.L. Feltri, unpublished observation). We propose that the Schwann cell response to P_0 overexpression further dysregulates the stoichiometry of myelin proteins (MBP and PMP22 are required for normal peripheral nerve myelination; Adlkofer et al., 1995; Gould et al., 1995; Martini et al., 1995), leading to reversible hypomyelination at the peak of P_0 gene expression in the third week after birth, and recovery as P_0 expression falls to adult levels. Parallel morphological and expression analysis throughout Tg80.3 nerve development will be required to test this hypothesis.

In contrast, the Schwann cells that are arrested at the stage of 1:1 relationships with axons deliver P_0 to atypical membrane locations. In Yin et al. (2000, this issue), we show that mistargeting of P_0 to the membranes of the advancing mesaxon activates obligate P_0 homophilic adhesion, arresting spiral wrapping and myelination.

Finally, many Schwann cells in the severely affected mice are unable to properly sort mixed caliber axons in spinal roots and nerves. P_0 was detected in these Schwann cells by immunocytochemistry (Yin et al., 2000, this issue). This sorting defect likely arises from P_0 overexpression rather than ectopic expression, as both P_0 mRNA and protein also have been detected in normal late embryonic nerves, when Schwann cell sorting of axons normally begins (Lee et al., 1997). Qualitative analysis of Schwann cell number (Fig. 3) and internuclear distance (Yin et al., 2000, this issue) in the severely affected nerves suggest that there is no defect in Schwann cell proliferation or survival, a conclusion that is also supported by BrdU-labeling indices (Yin, X., and B.D. Trapp, unpublished observation). This is in contrast to ErbB3 null mice, in which sciatic nerves contain bundles of unsorted axons due to a marked reduction in the number of Schwann cells (Riethmacher et al., 1997). Alternatively, as an adhesion molecule, P_0 may interfere with Schwann cell migration or elongation. In dystrophic (*dy/dy*) mice with laminin 2 deficiency, spinal nerves also contain bundles of naked, mixed caliber axons, hypothesized to be due to a Schwann cell migration defect (Madrid et al., 1975). Further studies of the cell growth and the molecular phenotype of the P_0 transgenic Schwann cells are underway to distinguish these possibilities.

P_0 Gene Dosage and Stoichiometry

Mutations in both P_0 and PMP22 result in similar dysmyelinating phenotypes, suggesting common functions. Recently, D'Urso et al. (1999) have provided biochemical evidence for physical interaction between P_0 and PMP22, suggesting the possibility of multiprotein assemblies in myelin. Determination of the crystal structure of the P_0 extracellular domain suggests that P_0 could interact with itself in compact myelin to form a planar crystal with regular spaces (Shapiro et al., 1996). Such spaces could potentially accommodate PMP22 (D'Urso et al., 1999) and define a fixed ratio between P_0 and PMP22 content. As noted above, the threshold of overexpression (80%) is remarkably similar for both P_0 (present study) and PMP22 (Huxley et al., 1998), a result that could be interpreted in terms of a fixed stoichiometry in their assembly. One prediction of such a model is that overexpression of one partner protein may perturb assembly through trans-dominant negative interactions with the other (e.g., sequestration or altering geometric interactions). Paradoxically, therefore, matching of the expression of partner proteins to comply with stoichiometric requirements may rescue dysmyelination, for example by crossing appropriate P_0- and PMP22-overexpressing mice. Such paradoxical rescue has been observed in CNS myelin when the shiverer phenotype (absence of MBP) was improved by reducing PLP dosage (Stoffel et al., 1997).

Implications for Hereditary Neuropathies

Increased dosage of PMP22 and PLP causes both rodent and human myelinopathies (CMT1A and Pelizeaus-Merzbacher Disease, respectively), and 80% overexpression of *Mpz* causes neuropathy in mice. Could altered dosage of *MPZ* cause human neuropathy? Partial trisomies of human chromosome 1 that include the *MPZ* locus 1q22 are rare and produce complex phenotypes; one such case included equinovarus alterations of the feet and contractures of the extremities, which suggest, but do not prove, peripheral neuropathy (Chen et al., 1994). Also, P_0 missense mutations are associated with the human demyelinating neuropathies CMT1B, Déjérine Sottas syndrome, and congenital hypomyelination neuropathy (CHN; Warner et al., 1996). Of note, profoundly reduced nerve conduction velocities (1–2 m/s), the paucity of active myelin destruction or onion bulbs, and the redundant basement membrane formation (Fig. 4 C) in P_0 overexpressor mice resemble CHN (Harati and Butler, 1985). In addition, low level P_0 overexpression produces transient hypomyelination in mice, similar to a subset of reversible CHN (Ghamdi et al., 1997; Levy et al., 1997). Finally, mutations in the Krox 20 transcription factor, encoded by *EGR2*, are also associated with CHN. Since one of these *EGR2* mutations likely disinhibits Krox 20 (Warner et al., 1998), and Krox 20 may regulate P_0 expression (Topilko et al., 1994; Zorick et al., 1999), it is possible that *MPZ* overexpression contributes to the pathogenesis of this *EGR2* mutation.

The present study advises caution for treatment of CMT1B neuropathies in which the *MPZ* mutation predicts loss of P_0 expression, and for which replacement gene therapy might therefore be considered (Shy et al., 1995; Guenard et al., 1999). Such therapy may require exceptionally precise regulation of P_0 expression in human nerve, as only 60% overexpression in mice results in impaired myelin formation.

Finally, Tg80.2 animals develop atrophy and morphologic changes in skeletal muscle, and a trend towards reduced nerve action potential amplitude, that together suggest axonal pathology. Axonal degeneration was not observed in studies of proximal nerves or lumbar ventral roots, but is prominent in intramuscular nerve branches (Yin, X., and B.D. Trapp, unpublished observations). It is well established from mouse models that primary defects in Schwann cells can lead to secondary changes in axonal properties (de Waegh et al., 1992; Yin et al., 1998), includ-

ing in distal nerves where axons might even be prone to degenerate (Frei et al., 1999; Sancho et al., 1999). Similarly, hereditary demyelinating neuropathies in man manifest important axonal effects, more prominent distally, which account for significant disability. Thus, mice overexpressing P_0 may provide another useful model for studying the pathogenesis of axonal damage as a consequence of primary Schwann cell dysfunction.

We thank Marta Arona, Marina Fasolini, Heide Peickert, Rita Numerato, and Denice Springman for expert technical assistance; Professor Melitta Schachner for the generous gift of P_0 null mice; Drs. Juan Archelos and Ueli Suter for the generous gifts of antibodies; and Professors Edoardo Boncinelli and Nicola Canal for support.

This study was supported by grants from Telethon, Italy (#1177 to L. Wrabetz, #D093 to M.L. Feltri); European Community Biomed Programme (#BMH-CT97-2069 to L. Wrabetz); Fondazione Giovanni Armenise-Harvard (L. Wrabetz and M.L. Feltri); and NIH (NS-23375 to S.Y. Chiu and A. Messing, and NS-38186 to B.D. Trapp).

Submitted: 19 October 1999
Revised: 13 January 2000
Accepted: 24 January 2000

References

Adlkofer, K., R. Martini, A. Aguzzi, J. Zielasek, K.V. Toyka, and U. Suter. 1995. Hypermyelination and demyelinating peripheral neuropathy in Pmp22-deficient mice. *Nat. Genet.* 11:274–280.

Archelos, J.J., K. Roggenbuck, J. Schneider-Schaulies, C. Linington, K.V. Toyka, and H.P. Hartung. 1993. Production and characterization of monoclonal antibodies to the extracellular domain of P_0. *J. Neurosci. Res.* 35:46–53.

Barbarese, E., J.H. Carson, and P. Braun. 1978. Accumulation of the four myelin basic proteins in mouse brain during development. *J. Neurochem.* 31: 779–782.

Bermingham, J.R., Jr., S.S. Scherer, S. O'Connell, E. Arroyo, K.A. Kalla, F.L. Powell, and M.G. Rosenfeld. 1996. Tst-1/Oct-6/SCIP regulates a unique step in peripheral myelination and is required for normal respiration. *Genes Dev.* 10:1751–1762.

Boison, D., and W. Stoffel. 1994. Disruption of the compacted myelin sheath of axons of the central nervous system in proteolipid protein-deficient mice. *Proc. Natl. Acad. Sci. USA.* 91:11709–11713.

Brinster, R.L., H.Y. Chen, M.E. Trumbauer, M.K. Yagle, and R.D. Palmiter. 1985. Factors affecting the efficiency of introducing foreign DNA into mice by microinjecting eggs. *Proc. Natl. Acad. Sci. USA.* 82:4438–4442.

Brunden, K.R. 1992. Age-dependent changes in the oligosaccharide structure of the major myelin glycoprotein, P_0. *J. Neurochem.* 58:1659–1666.

Chen, H., C.J. Kusyk, C.M. Tuck-Muller, J.E. Martinez, R.D. Dorand, and W. Wertelecki. 1994. Confirmation of proximal 1q duplication using fluorescence in situ hybridization. *Am. J. Med. Genet.* 50:28–31.

Chirgwin, J.M., A.E. Przbyla, R.J. MacDonald, and R.J. Rutter. 1979. Isolation of biologically active ribonucleic acid from sources enriched in ribonuclease. *Biochemistry.* 18:5294–5299.

Colman, D.R., G. Kreibich, A.B. Frey, and D.D. Sabatini. 1982. Synthesis and incorporation of myelin polypeptides into CNS myelin. *J. Cell Biol.* 95:598–608.

D'Urso, D., P.J. Brophy, S.M. Staugaitis, C.S. Gillespie, A.B. Frey, J.G. Stempak, and D.R. Colman. 1990. Protein zero of peripheral nerve myelin: biosynthesis, membrane insertion, and evidence for homotypic interaction. *Neuron.* 4:449–460.

D'Urso, D., P. Ehrhardt, and H.W. Muller. 1999. Peripheral myelin protein 22 and protein zero: a novel association in peripheral nervous system myelin. *J. Neurosci.* 19:3396–3403.

de Waegh, S.M., V.M. Lee, and S.T. Brady. 1992. Local modulation of neurofilament phosphorylation, axonal caliber, and slow axonal transport by myelinating Schwann cells. *Cell.* 68:451–463.

Feltri, M.L., M. D'Antonio, A. Quattrini, R. Numerato, M. Arona, S. Previtali, S.Y. Chiu, A. Messing, and L. Wrabetz. 1999. A novel P_0 glycoprotein transgene activates expression of *lac*Z in myelin-forming Schwann cells. *Eur. J. Neurosci.* 11:1577–1586.

Filbin, M.T., F.S. Walsh, B.D. Trapp, J.A. Pizzey, and G.I. Tennekoon. 1990. Role of myelin P_0 protein as a homophilic adhesion molecule. *Nature.* 344: 871–872.

Frei, R., S. Motzing, I. Kinkelin, M. Schachner, M. Koltzenburg, and R. Martini. 1999. Loss of distal axons and sensory Merkel cells and features indicative of muscle denervation in hindlimbs of P_0-deficient mice. *J. Neurosci.* 19: 6058–6067.

Ghamdi, M., D.L. Armstrong, and G. Miller. 1997. Congenital hypomyelinating neuropathy: a reversible case. *Pediatr. Neurol.* 16:71–73.

Giese, K.P., R. Martini, G. Lemke, P. Soriano, and M. Schachner. 1992. Mouse P_0 gene disruption leads to hypomyelination, abnormal expression of recognition molecules, and degeneration of myelin and axons. *Cell.* 71:565–576.

Gould, R.M., A.L. Byrd, and E. Barbarese. 1995. The number of Schmidt-Lanterman incisures is more than doubled in shiverer PNS myelin sheaths. *J. Neurocytol.* 24:85–98.

Greenfield, S., S. Brostoff, E.H. Eylar, and P. Morell. 1973. Protein composition of myelin of the peripheral nervous system. *J. Neurochem.* 20:1207–1216.

Griffiths, I.R., L.S. Mitchell, K. McPhilemy, S. Morrison, E. Kyriakides, and J.A. Barrie. 1989. Expression of myelin protein genes in Schwann cells. *J. Neurocytol.* 18:345–352.

Guenard, V., B. Schweitzer, E. Flechsig, S. Hemmi, R. Martini, U. Suter, and M. Schachner. 1999. Effective gene transfer of lacZ and P_0 into Schwann cells of P_0-deficient mice. *Glia.* 25:165–178.

Harati, Y., and I.J. Butler. 1985. Congenital hypomyelinating neuropathy. *J. Neurol. Neurosurg. Psychiatry.* 48:1269–1276.

Huxley, C., E. Passage, A.M. Robertson, B. Youl, S. Huston, A. Manson, D. Saberan-Djoniedi, D. Figarella-Branger, J.F. Pellissier, P.K. Thomas, and M. Fontes. 1998. Correlation between varying levels of PMP22 expression and the degree of demyelination and reduction in nerve conduction velocity in transgenic mice. *Hum. Mol. Genet.* 7:449–458.

Jaegle, M., W. Mandemakers, L. Broos, R. Zwart, A. Karis, P. Visser, F. Grosveld, and D. Meijer. 1996. The POU factor Oct-6 and Schwann cell differentiation. *Science.* 273:507–510.

Kagawa, T., K. Ikenaka, Y. Inoue, S. Kuriyama, T. Tsujii, J. Nakao, K. Nakajima, J. Aruga, H. Okano, and K. Mikoshiba. 1994. Glial cell degeneration and hypomyelination caused by overexpression of myelin proteolipid protein gene. *Neuron.* 13:427–442.

Klugmann, M., M.H. Schwab, A. Puhlhofer, A. Schneider, F. Zimmermann, I.R. Griffiths, and K.A. Nave. 1997. Assembly of CNS myelin in the absence of proteolipid protein. *Neuron.* 18:59–70.

Lee, M.-J., A. Brennan, A. Blanchard, G. Zoidl, Z. Dong, A. Tabernero, C. Zoidl, M.A.R. Dent, K.R. Jessen, and R. Mirsky. 1997. P_0 is constitutively expressed in the rat neural crest and embryonic nerves and is negatively and positively regulated by axons to generate non-myelin-forming and myelin-forming Schwann cells, respectively. *Mol. Cell. Neurosci.* 8:336–350.

Lemke, G., and R. Axel. 1985. Isolation and sequence of a cDNA encoding the major structural protein of peripheral myelin. *Cell.* 40:501–508.

Levy, B.K., G.A. Fenton, S. Loaiza, and G.R. Hayat. 1997. Unexpected recovery in a newborn with severe hypomyelinating neuropathy. *Pediatr. Neurol.* 16:245–248.

Madrid, R.E., E. Jaros, M.J. Cullen, and W.G. Bradley. 1975. Genetically determined defect of Schwann cell basement membrane in dystrophic mouse. *Nature.* 257:319–321.

Magyar, J.P., R. Martini, T. Ruelicke, A. Aguzzi, K. Adlkofer, Z. Dembic, J. Zielasek, K.V. Toyka, and U. Suter. 1996. Impaired differentiation of Schwann cells in transgenic mice with increased PMP22 gene dosage. *J. Neurosci.* 16:5351–5360.

Martini, R. 1997. Animal models for inherited peripheral neuropathies. *J. Anat.* 191:321–336.

Martini, R., M. Mohajeri, S. Kasper, K. Giese, and M. Schachner. 1995. Mice doubly deficient in the genes for P_0 and myelin basic protein show that both proteins contribute to the formation of the major dense line in peripheral nerve myelin. *J. Neurosci.* 15:4488–4495.

Nave, K.A., and O. Boespflug-Tanguy. 1996. X-linked developmental defects of myelination: from mouse mutants to human genetic diseases. *Neuroscientist.* 2:33–43.

Norton, W.T., and S.E. Poduslo. 1973. Myelination in rat brain: changes in myelin composition during brain maturation. *J. Neurochem.* 21:759–773.

Quattrini, A., S. Previtali, M.L. Feltri, N. Canal, R. Nemni, and L. Wrabetz. 1996. Beta 4 integrin and other Schwann cell markers in axonal neuropathy. *Glia.* 17:294–306.

Readhead, C., A. Schneider, I. Griffiths, and K.A. Nave. 1994. Premature arrest of myelin formation in transgenic mice with increased proteolipid protein gene dosage. *Neuron.* 12:583–595.

Riethmacher, D., E. Sonnenberg-Riethmacher, V. Brinkmann, T. Yamaai, G.R. Lewin, and C. Birchmeier. 1997. Severe neuropathies in mice with targeted mutations in the ErbB3 receptor. *Nature.* 389:725–730.

Sambrook, J., E.F. Fritsch, and T. Maniatis. 1989. Molecular Cloning. Cold Spring Harbor Laboratory Press, Cold Spring Harbor, NY.

Sancho, S., J.P. Magyar, A. Aguzzi, and U. Suter. 1999. Distal axonopathy in peripheral nerves of PMP22-mutant mice. *Brain.* 122:1563–1577.

Scherer, S.S., P.E. Braun, J. Grinspan, E. Collarini, D.Y. Wang, and J. Kamholz. 1994. Differential regulation of the 2′,3′-cyclic nucleotide 3′-phosphodiesterase gene during oligodendrocyte development. *Neuron.* 12:1363–1375.

Schneider-Schaulies, J., A. von Brunn, and M. Schachner. 1990. Recombinant peripheral myelin protein P_0 confers both adhesion and neurite outgrowth-promoting properties. *J. Neurosci. Res.* 27:286–297.

Sereda, M., I. Griffiths, A. Puhlhofer, H. Stewart, M.J. Rossner, F. Zimmermann, J.P. Magyar, A. Schneider, E. Hund, H.M. Meinck, et al. 1996. A transgenic rat model of Charcot-Marie-Tooth disease. *Neuron.* 16:1049–1060.

Shapiro, L., J.P. Doyle, P. Hensley, D.R. Colman, and W.A. Hendrickson. 1996. Crystal structure of the extracellular domain from P_0, the major struc-

tural protein of peripheral nerve myelin. *Neuron.* 17:435–449.
Shy, M.E., M. Tani, Y.J. Shi, S.A. Whyatt, T. Chbihi, S.S. Scherer, and J. Kamholz. 1995. An adenoviral vector can transfer *lac*Z expression into Schwann cells in culture and in sciatic nerve. *Ann. Neurol.* 38:429–436.
Stahl, N., J. Harry, and B. Popko. 1990. Quantitative analysis of myelin protein gene expression during development in the rat sciatic nerve. *Mol. Brain. Res.* 8:209–212.
Stoffel, W., D. Boison, and H. Bussow. 1997. Functional analysis in vivo of the double mutant mouse deficient in both proteolipid protein (PLP) and myelin basic protein (MBP) in the central nervous system. *Cell Tissue Res.* 289: 195–206.
Suter, U., and G.J. Snipes. 1995. Biology and genetics of hereditary motor and sensory neuropathies. *Annu. Rev. Neurosci.* 18:45–75.
Topilko, P., S. Schneider-Maunoury, G. Levi, A. Baron-Van Evercooren, A.B. Chennoufi, T. Seitanidou, C. Babinet, and P. Charnay. 1994. Krox-20 controls myelination in the peripheral nervous system. *Nature.* 371:796–799.
Trapp, B.D., T. Moench, M. Pulley, E. Barbosa, G. Tennekoon, and J. Griffin. 1987. Spatial segregation of mRNA encoding myelin-specific proteins. *Proc. Natl. Acad. Sci. USA.* 84:7773–7777.
Trapp, B.D., G.J. Kidd, P. Hauer, E. Mulrenin, C.A. Haney, and S.B. Andrews. 1995. Polarization of myelinating Schwann cell surface membranes: role of microtubules and the trans-Golgi network. *J. Neurosci.* 15:1797–1807.
Ueyama, T. 1978. The topography of root fibres within the sciatic nerve trunk of the dog. *J. Anat.* 127:277–290.
Vallat, J.M., P. Sindou, P.M. Preux, F. Tabaraud, A.M. Milor, P. Couratier, E. LeGuern, and A. Brice. 1996. Ultrastructural PMP22 expression in inherited demyelinating neuropathies. *Ann. Neurol.* 39:813–817.
Warner, L.E., M.J. Hilz, S.H. Appel, J.M. Killian, E.H. Kolodny, G. Karpati, S. Carpenter, G.V. Watters, C. Wheeler, D. Witt, et al. 1996. Clinical phenotypes of different *MPZ* (P_0) mutations may include Charcot-Marie-Tooth Type 1b, Dejerine-Sottas, and congenital hypomyelination. *Neuron.* 17:451–460.
Warner, L.E., P. Mancias, I.J. Butler, C.M. McDonald, L. Keppen, K.G. Koob, and J.R. Lupski. 1998. Mutations in the early growth response 2 (*EGR2*) gene are associated with hereditary myelinopathies. *Nat. Genet.* 18:382–384.
Werner, H., M. Jung, M. Klugmann, M. Sereda, I.R. Griffiths, and K.A. Nave. 1998. Mouse models of myelin diseases. *Brain Pathol.* 8:771–793.
Wrabetz, L., C. Taveggia, M. Feltri, A. Quattrini, R. Awatramani, S. Scherer, A. Messing, and J. Kamholz. 1998. A minimal human MBP promoter-*lacZ* transgene is appropriately regulated in developing brain and after optic enucleation, but not in shiverer mutant mice. *J. Neurobiol.* 34:10–26.
Yin, X., T.O. Crawford, J.W. Griffin, P. Tu, V.M. Lee, C. Li, J. Roder, and B.D. Trapp. 1998. Myelin-associated glycoprotein is a myelin signal that modulates the caliber of myelinated axons. *J. Neurosci.* 18:1953–1962.
Yin, X., G. Kidd, L. Wrabetz, M. Feltri, A. Messing, and B. Trapp. 2000. Schwann cell myelination requires timely and precise targeting of P_0 protein. *J. Cell Biol.* 148:1009–1020.
Zorick, T.S., D.E. Syroid, A. Brown, T. Gridley, and G. Lemke. 1999. Krox-20 controls SCIP expression, cell cycle exit and susceptibility to apoptosis in developing myelinating Schwann cells. *Development.* 126:1397–1406.